

Supporting Information for

**Zirconium Metal-organic Cage Decorated with Squaramides
Imparts Dual Activation for Chemical Fixation of CO₂
under Mild Conditions**

Xiaoli Zhao,^a Yue Tang,^a Yuxuan Wang,^a Xinjing Rong,^a Pengyan Wu,*^a Zihan Li,^a
Ning Cai,^a Xinyi Deng^a and Jian Wang*^a

^a Jiangsu Key Laboratory of Green Synthetic Chemistry for Functional Materials,
School of Chemistry and Materials Science, Jiangsu Normal University, Xuzhou,
221116, P. R. China.

E-mail: wpyan@jsnu.edu.cn; wjian@jsnu.edu.cn

Materials and Methods

Reagents and chemicals: All reagents and solvents were of AR grade and used without further purification unless otherwise noted. 4,4'-(3,4-dioxocyclobut-1-ene-1,2-diyl)bis(azanediyl) dibenzoic acid was synthesized according to the literature methods.^{S1} Zirconocene dichloride was purchased from Shanghai Aladdin Biochemical Technology Co., Ltd. All of the epoxides (epibromohydrin, epichlorohydrin, propylene oxide, epoxybutane, glycidol, allyl glycidyl ether, butyl glycidyl ether, glycidyl phenyl ether, 4-*tert*-butylphenyl glycidyl ether and Tetrabutylammonium Bromide (TBAB) were purchased from Beijing Innochem Science & Technology Co., Ltd.

Instruments and spectroscopic measurements: The elemental analyses of C, H and N were performed on a Vario EL III elemental analyzer. ¹H NMR spectra were measured on a Bruker-400 spectrometer with Me₄Si as an internal standard. X-Ray powder diffraction (XRD) patterns of the Zr-DBDA was recorded on a Rigaku D/max-2400 X-ray powder diffractometer (Japan) using Cu-K α ($\lambda = 1.5405 \text{ \AA}$) radiation. FT-IR spectra were recorded as KBr pellets on JASCO FT/IR-430. Thermogravimetric analysis (TGA) was carried out at a ramp rate of 5 °C/min in a nitrogen flow with a Rigaku Thermo plus TG-8120 instrument. The morphologies of the prepared samples were recorded by a Field Emission Scanning Electron Microscopy (SEM) of Hitachi SU8010. Samples were treated via Pt sputtering for 90 s before observation. The contents of metal ions were measured by inductively coupled plasma mass spectrometry (ICP-MS; Leeman PROFILE SPEC).

Experimental

Synthesis of Zr-DBDA·4DEF: 4,4'-(3,4-dioxocyclobut-1-ene-1,2-diyl)bis(azanediyl)dibenzoic acid (H₂dbda) (21 mg, 0.06 mmol) and zirconocene dichloride (35 mg, 0.12 mmol) were dissolved in 6 mL N,N-Diethylformamide/water in a screw-capped vial. The resulting mixture was placed in an oven at 60°C for 12 hours; upon cooling, light yellow block crystals were collected by filtration. Yield: 73%.

Anal calc. for $\{[\text{Cp}_3\text{Zr}_3(\mu_3\text{-O})(\mu_2\text{-OH})_3]_2(\text{DBDA})_3\} \cdot \text{Cl}_2 \cdot 4\text{DEF} \cdot 8\text{H}_2\text{O}$: C 45.55, H 4.63, N 5.11%; Found: C 45.62, H 4.59, N 5.03%.

Typical Procedure for the Reaction of CO₂ Cycloaddition of Epoxides: The catalytic reaction was conducted in a glass reaction tube, which was purged with 1 atm CO₂ under constant pressure for 15 min to allow the system equilibration. The vessel was set on an agitator with frequent stirring at room temperature for 10 h. At the end of the reaction, the catalysts were separated through centrifugation, and a small aliquot of the supernatant reaction mixture was analyzed by ¹H NMR to calculate the reaction yields.

Recyclability of Zr-DBDA. The recyclability experiment for the reaction of CO₂ cycloaddition of epoxides was carried out under the similar reaction conditions. The catalyst was retrieved by filtration, washed with chloroform, and heated at 150°C under vacuum for 6 h to regenerate the active catalyst, before it was used for the next catalytic cycle.

X-ray Crystallography (Single-crystal diffraction).

Crystal data of Zr–DBDA·4DEF:

$C_{104}H_{110}Cl_2N_{10}O_{30}Zr_6$, Mr = 2598.23, Triclinic, space group $P\ -1$, $a = 14.5715(15)$, $b = 15.2988(16)$, $c = 27.002(3)$ Å, $\alpha = 79.0630(10)$, $\beta = 76.5090(10)$, $\gamma = 82.186(2)$ °, $V = 5720.4(10)$ Å³, $Z = 2$, $D_c = 1.508$ g cm⁻³, $\mu(\text{Mo-K}\alpha) = 0.651$ mm⁻¹, T = 296(2) K. 15088 unique reflections [$R_{\text{int}} = 0.0249$]. Final R_I [with $I > 2\sigma(I)$] = 0.0587, wR_2 (all data) = 0.1805, GOOF = 1.068. CCDC number: 2266537.

Crystallography:

Intensities were collected on a Bruker SMART APEX CCD diffractometer with graphitemonochromated Mo-K α ($\lambda = 0.71073$ Å) using the SMART and SAINT programs. The structure was solved by direct methods and refined on F^2 by full-matrix least-squares methods with SHELXTL *version 5.1*. Non-hydrogen atoms of the ligand backbones were refined anisotropically. Hydrogen atoms within the ligand backbones were fixed geometrically at calculated positions and allowed to ride on the parent non-hydrogen atoms. The lattice solvents were confirmed according to TGA data and elemental analysis, and the data were treated with the SQUEEZE routine within PLATON.

Table S1 Selective bond distance (\AA) and angle ($^\circ$) in Zr–DBDA·4DEF.

Zr(1)–O(5W)	2.074(3)	Zr(1)–O(6W)	2.119(4)
Zr(1)–O(7W)	2.153(4)	Zr(1)–O(10)	2.175(4)
Zr(1)–O(7)	2.185(4)	Zr(2)–O(5W)	2.086(3)
Zr(2)–O(6W)	2.130(4)	Zr(2)–O(8W)	2.137(4)
Zr(2)–O(8)	2.170(4)	Zr(2)–O(11)	2.184(4)
Zr(3)–O(4W)	2.071(3)	Zr(3)–O(2W)	2.126(4)
Zr(3)–O(3W)	2.137(4)	Zr(3)–O(18)	2.174(4)
Zr(3)–O(15)	2.233(4)	Zr(4)–O(4W)	2.084(4)
Zr(4)–O(3W)	2.118(4)	Zr(4)–O(1W)	2.119(4)
Zr(4)–O(13)	2.172(4)	Zr(4)–O(17)	2.181(4)
Zr(5)–O(5W)	2.073(3)	Zr(5)–O(8W)	2.140(4)
Zr(5)–O(7W)	2.146(4)	Zr(5)–O(12)	2.171(4)
Zr(5)–O(9)	2.203(4)	Zr(6)–O(4W)	2.077(4)
Zr(6)–O(1W)	2.118(4)	Zr(6)–O(2W)	2.127(4)
Zr(6)–O(16)	2.159(4)	Zr(6)–O(14)	2.185(4)
O(5W)–Zr(1)–O(6W)	73.75(13)	O(5W)–Zr(1)–O(7W)	73.26(13)
O(6W)–Zr(1)–O(7W)	89.30(14)	O(5W)–Zr(1)–O(10)	79.70(13)
O(6W)–Zr(1)–O(10)	153.19(14)	O(10)–Zr(1)–O(7)	84.71(14)
O(7W)–Zr(1)–O(10)	86.56(14)	O(5W)–Zr(1)–O(7)	79.62(13)
O(6W)–Zr(1)–O(7)	86.94(14)	O(7W)–Zr(1)–O(7)	152.59(14)
O(5W)–Zr(2)–O(6W)	73.28(13)	O(5W)–Zr(2)–O(8W)	72.95(13)
O(6W)–Zr(2)–O(8W)	89.84(14)	O(5W)–Zr(2)–O(8)	81.35(14)
O(6W)–Zr(2)–O(8)	85.20(14)	O(8W)–Zr(2)–O(8)	154.17(14)
O(5W)–Zr(2)–O(11)	78.35(13)	O(6W)–Zr(2)–O(11)	150.99(14)
O(8W)–Zr(2)–O(11)	87.54(14)	O(8)–Zr(2)–O(11)	84.71(14)
O(4W)–Zr(3)–O(2W)	73.46(13)	O(4W)–Zr(3)–O(3W)	73.21(14)
O(2W)–Zr(3)–O(3W)	89.52(15)	O(4W)–Zr(3)–O(18)	79.48(13)

O(2W)–Zr(3)–O(18)	152.61(14)	O(3W)–Zr(3)–O(18)	86.71(14)
O(4W)–Zr(3)–O(15)	79.39(14)	O(2W)–Zr(3)–O(15)	87.54(14)
O(3W)–Zr(3)–O(15)	152.13(14)	O(18)–Zr(3)–O(15)	83.32(14)
O(4W)–Zr(4)–O(3W)	73.35(14)	O(4W)–Zr(4)–O(1W)	73.13(14)
O(3W)–Zr(4)–O(1W)	90.38(15)	O(4W)–Zr(4)–O(13)	79.87(14)
O(3W)–Zr(4)–O(13)	153.03(15)	O(1W)–Zr(4)–O(13)	84.81(15)
O(4W)–Zr(4)–O(17)	79.04(14)	O(3W)–Zr(4)–O(17)	86.85(14)
O(1W)–Zr(4)–O(17)	151.63(15)	O(13)–Zr(4)–O(17)	85.00(15)
O(5W)–Zr(5)–O(8W)	73.15(13)	O(5W)–Zr(5)–O(7W)	73.43(13)
O(8W)–Zr(5)–O(7W)	88.77(14)	O(5W)–Zr(5)–O(12)	78.91(13)
O(8W)–Zr(5)–O(12)	86.62(14)	O(7W)–Zr(5)–O(12)	152.10(14)
O(5W)–Zr(5)–O(9)	79.67(13)	O(8W)–Zr(5)–O(9)	152.51(14)
O(7W)–Zr(5)–O(9)	87.38(14)	O(12)–Zr(5)–O(9)	84.19(14)
O(4W)–Zr(6)–O(1W)	73.28(14)	O(4W)–Zr(6)–O(2W)	73.32(13)
O(1W)–Zr(6)–O(2W)	90.74(15)	O(4W)–Zr(6)–O(16)	79.57(14)
O(1W)–Zr(6)–O(16)	152.45(15)	O(2W)–Zr(6)–O(16)	85.88(14)
O(4W)–Zr(6)–O(14)	79.74(14)	O(1W)–Zr(6)–O(14)	85.76(15)
O(2W)–Zr(6)–O(14)	152.68(14)	O(16)–Zr(6)–O(14)	84.88(14)

Figure S1 The asymmetry unit of Zr–DBDA·4DEF.

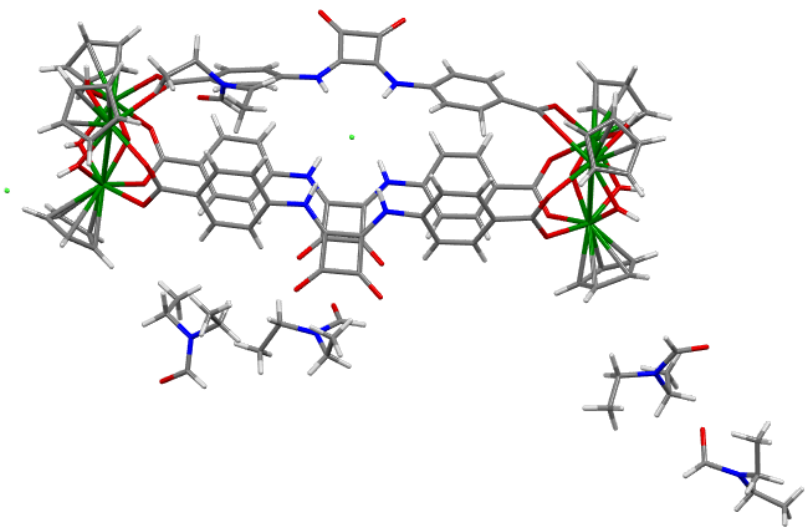


Figure S2 The three-dimensional spatial structure of the Zr–DBDA·4DEF.

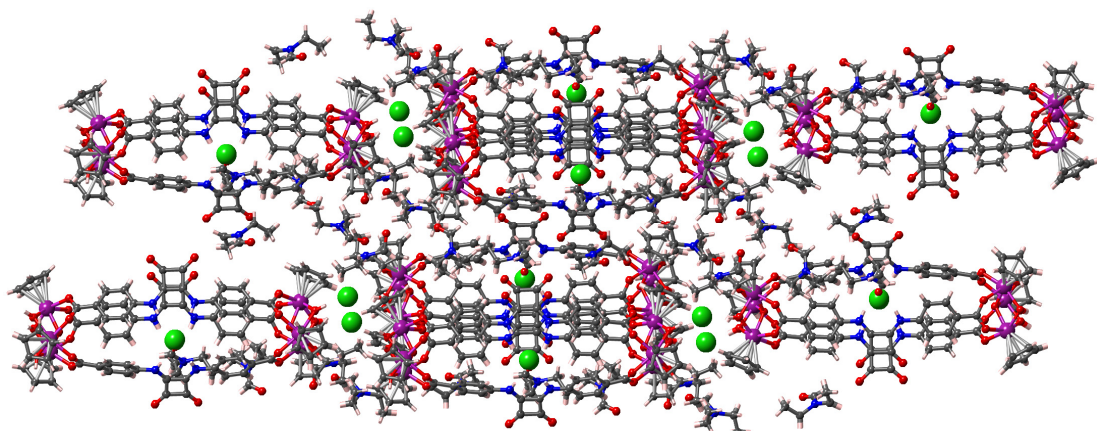


Figure S3 TGA traces of Zr–DBDA·4DEF and Zr–DBDA ranging from room temperature to 800 °C.

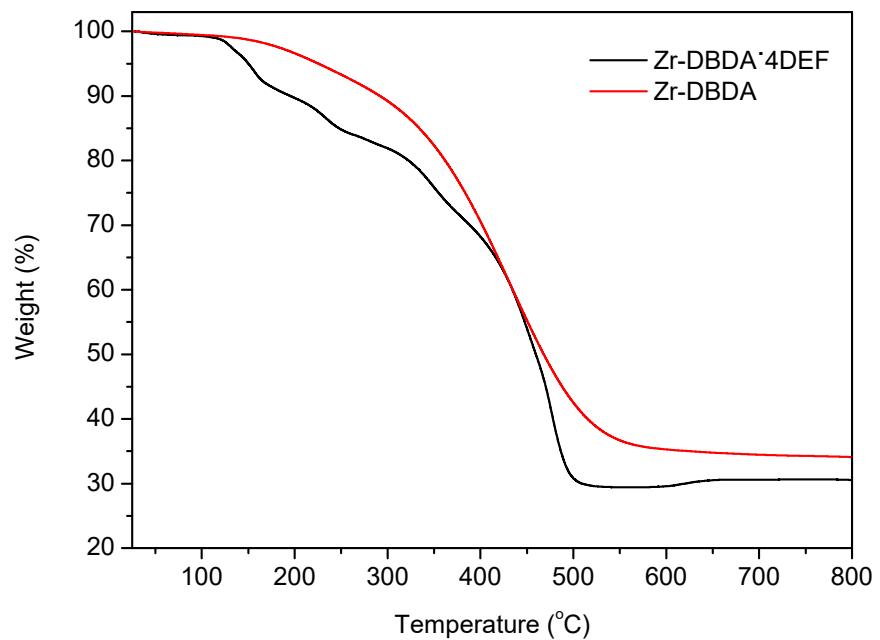


Figure S4 FT-IR spectra of Zr–DBDA·4DEF and Zr–DBDA.

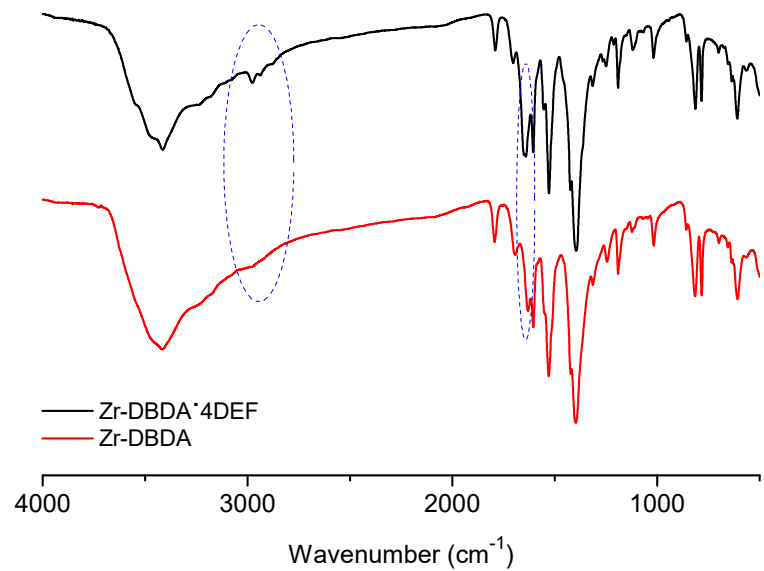


Figure S5 The XPS spectra of Zr–DBDA·4DEF and Zr–DBDA.

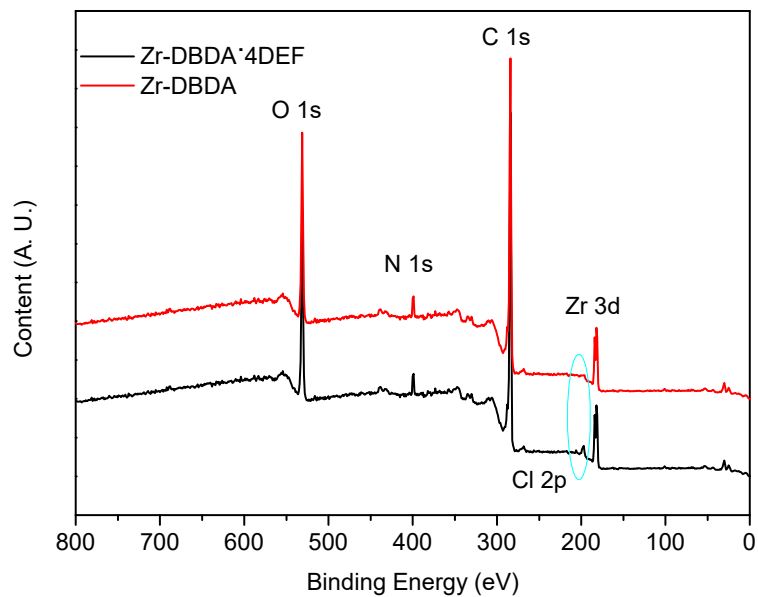


Figure S6 N₂ adsorption and desorption isotherms for Zr-DBDA at 77 K.

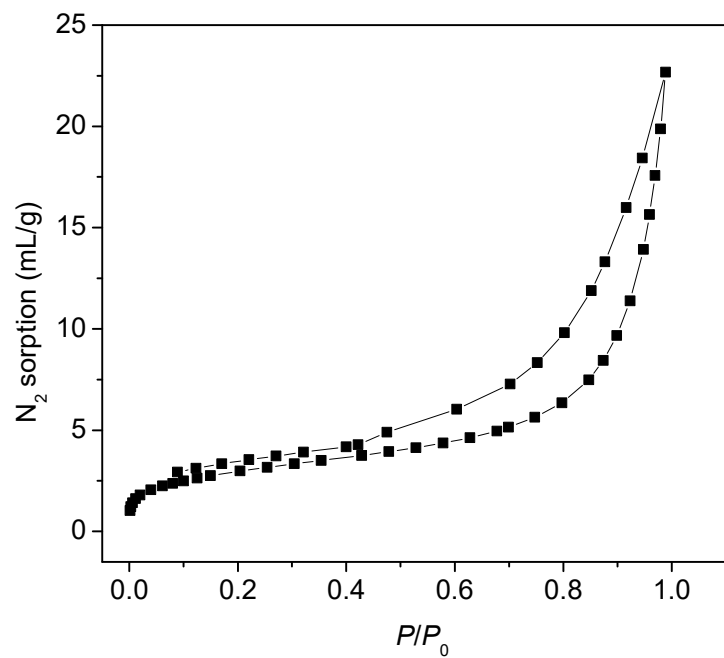
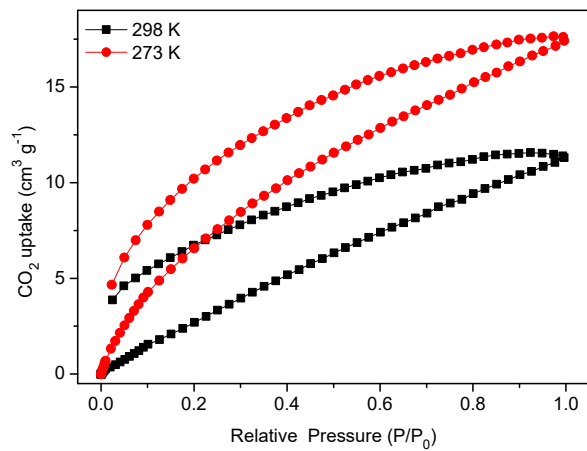
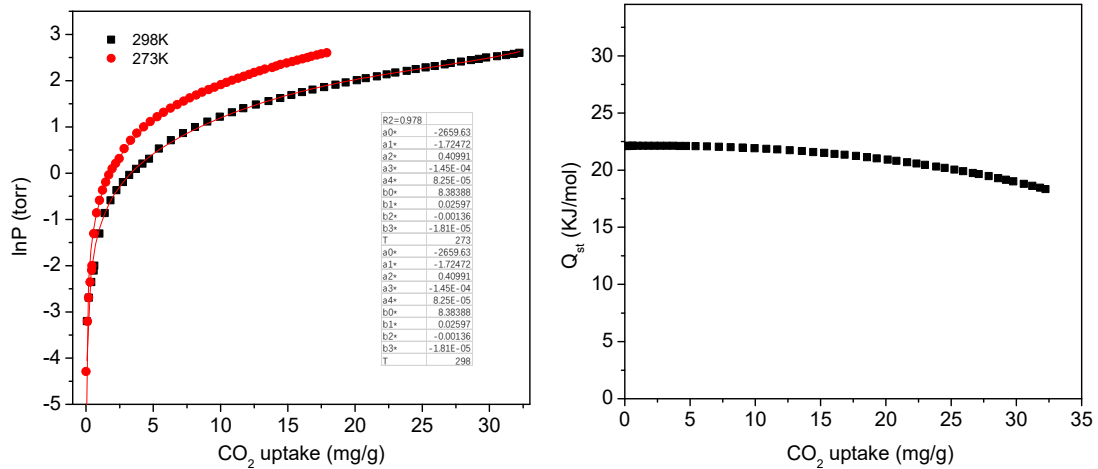


Figure S7 (a) CO₂ adsorption and desorption isotherms for Zr-DBDA at 273 and 298 K, respectively. (b) Nonlinear curve fitting of CO₄ adsorption isotherms for Zr-DBDA at 273 K and 298 K. (c) The heat of sorption for Zr-DBDA.



(a)



(b)

(c)

Figure S8 Recycling experiment of Zr-DBDA for CO₂ cycloaddition with EBH.

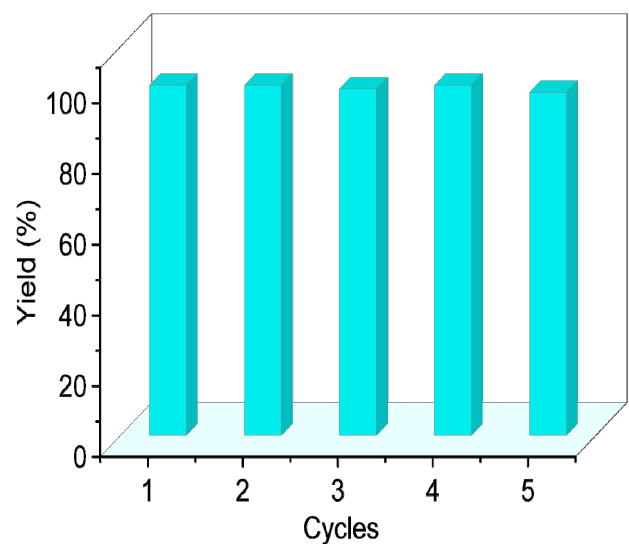


Figure S9 Powder XRD patterns of the simulation from Zr-DBDA·4DEF single-crystal data, the as-synthesized Zr-DBDA, Zr-DBDA after the 5th catalysis.

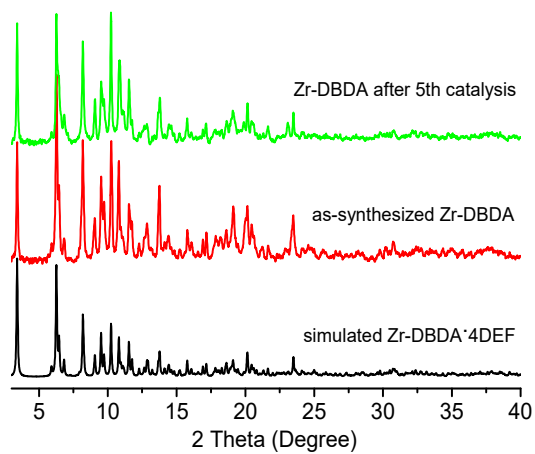


Figure S10 ^1H NMR (400 MHz, CDCl_3) for the yield of 4-(bromomethyl)-1,3-dioxolan-2-one.

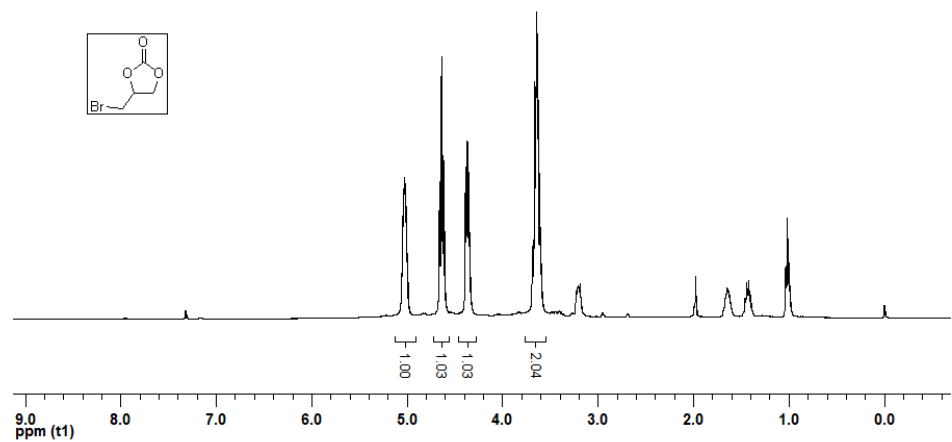


Figure S11 ^1H NMR (400 MHz, CDCl_3) for the yield of 4-(chloromethyl)-1,3-dioxolan-2-one.

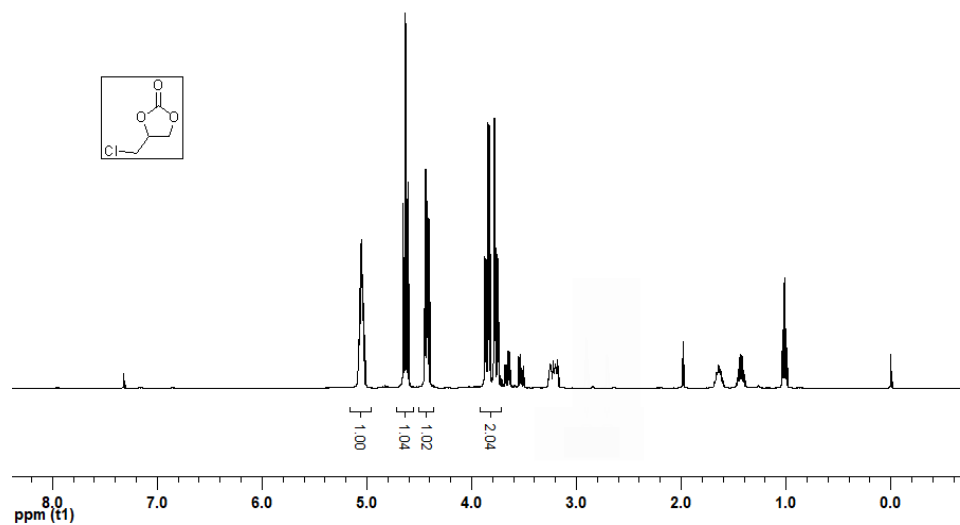


Figure S12 ^1H NMR (400 MHz, CDCl_3) for the yield of 4-methyl-1,3-dioxolan-2-one.

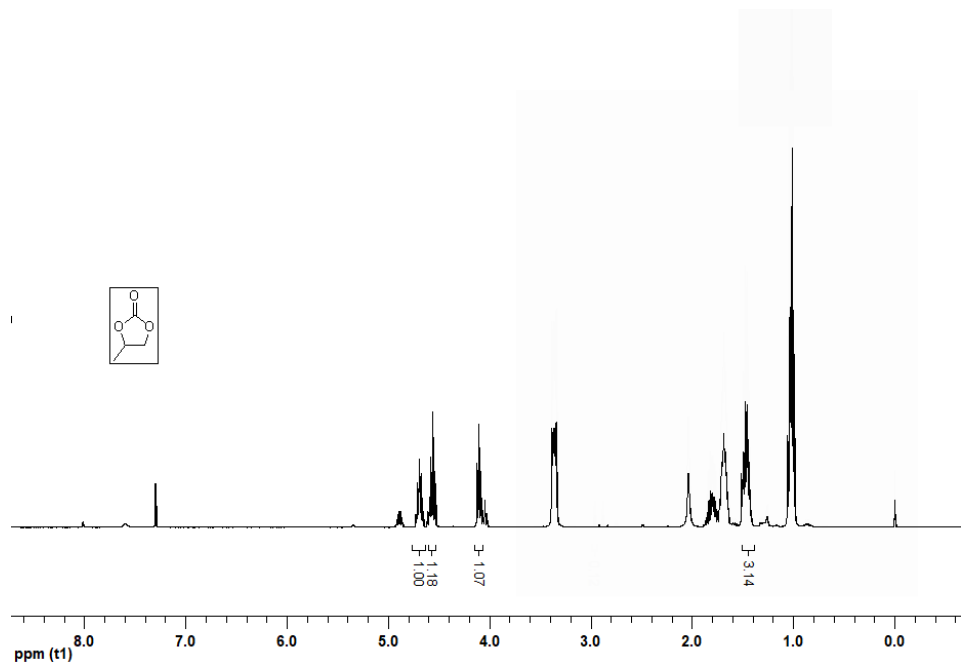


Figure S13 ^1H NMR (400 MHz, CDCl_3) for the yield of 4-ethyl-1,3-dioxolan-2-one.

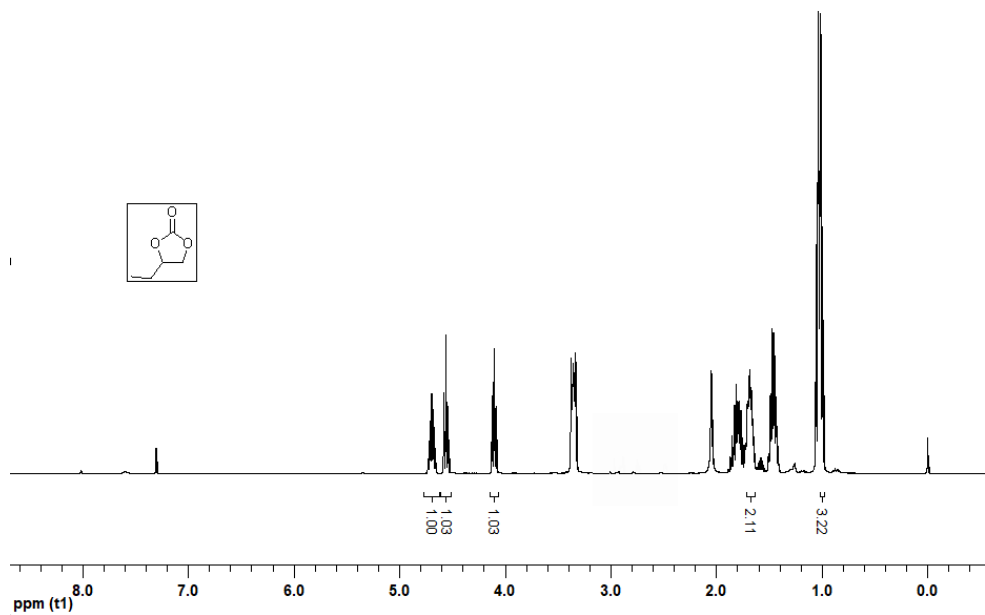


Figure S14 ^1H NMR (400 MHz, CDCl_3) for the yield of 4-(hydroxymethyl)-1,3-dioxolan-2-one.

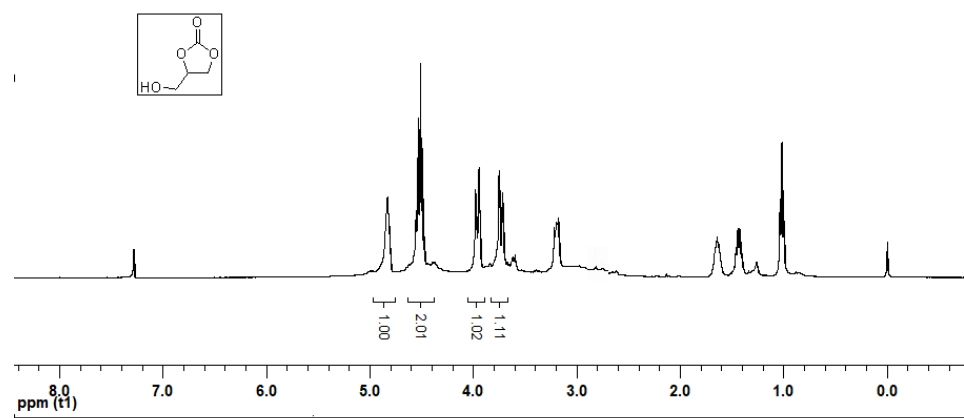


Figure S15 ^1H NMR (400 MHz, CDCl_3) for the yield of 4-((allyloxy)methyl)-1,3-dioxolan-2-one.

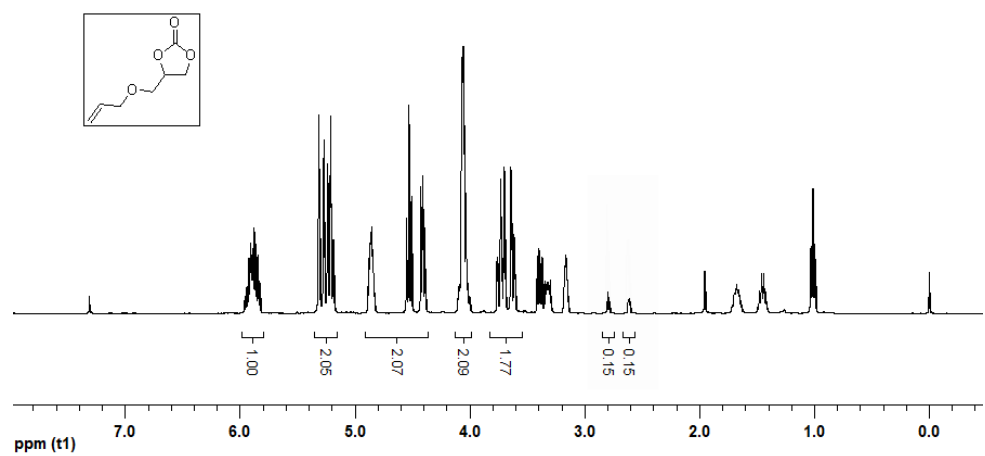


Figure S16 ^1H NMR (400 MHz, CDCl_3) for the yield of 4-(butoxymethyl)-1,3-dioxolan-2-one.

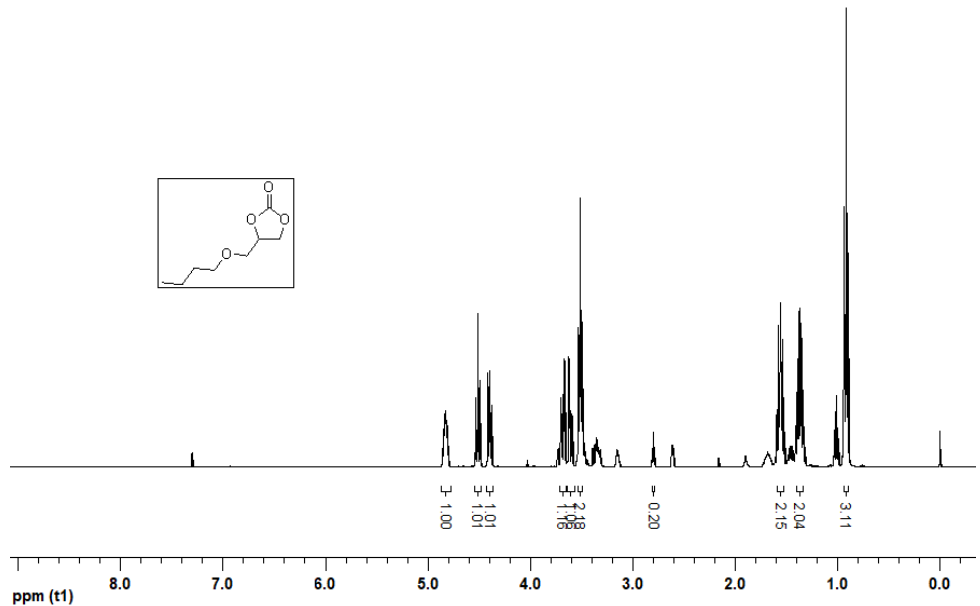


Figure S17 ^1H NMR (400 MHz, CDCl_3) for the yield of 4-(phenoxymethyl)-1,3-dioxolan-2-one.

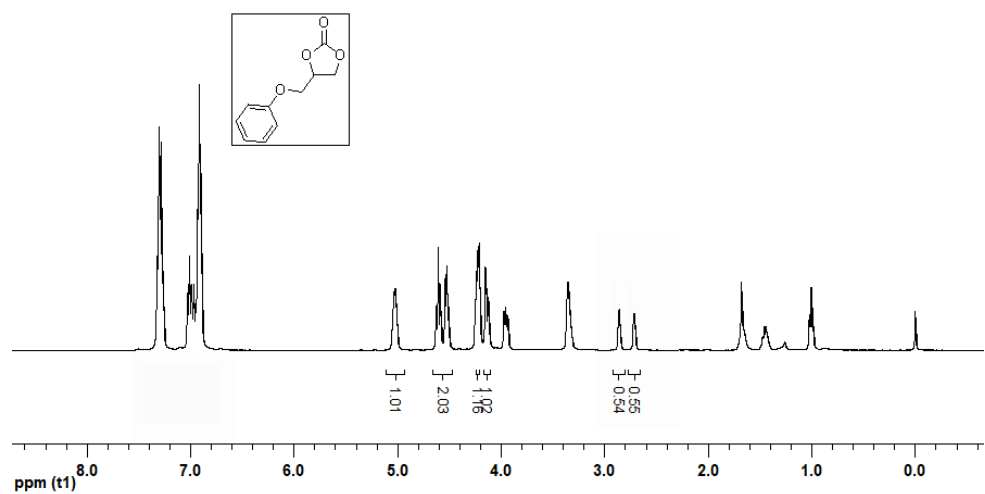


Figure S18 ^1H NMR (400 MHz, CDCl_3) for the yield of 4-((4-(tert-butyl)phenoxy)methyl)-1,3-dioxolan-2-one.

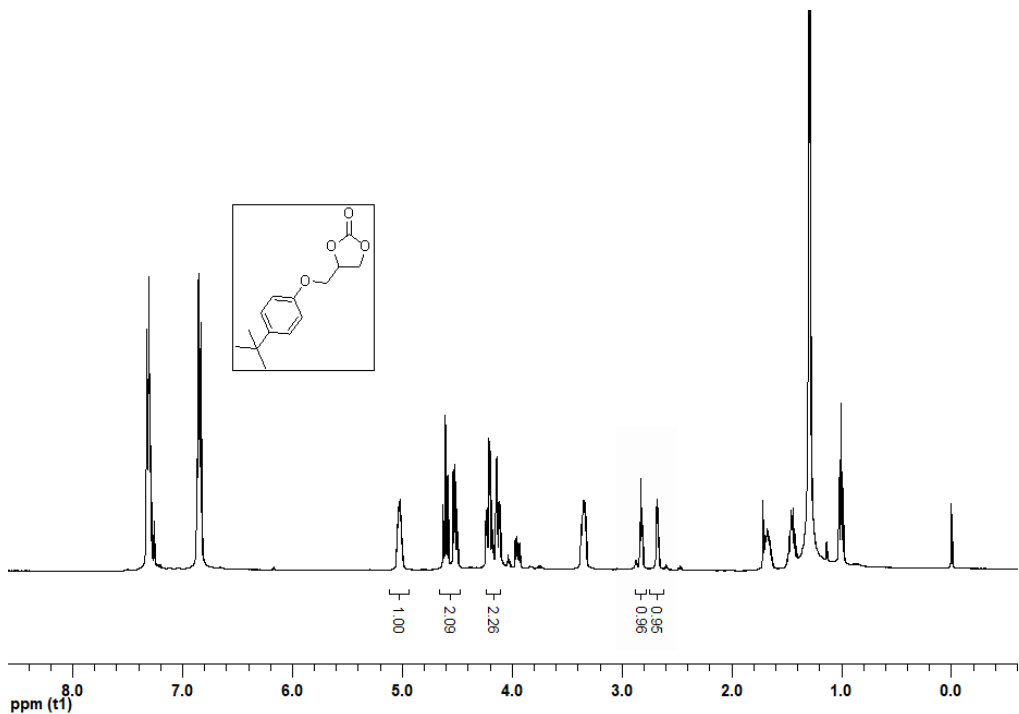


Figure S19 SEM image of Zr–DBDA and Zr–DBDA after 5th catalytic cycles.

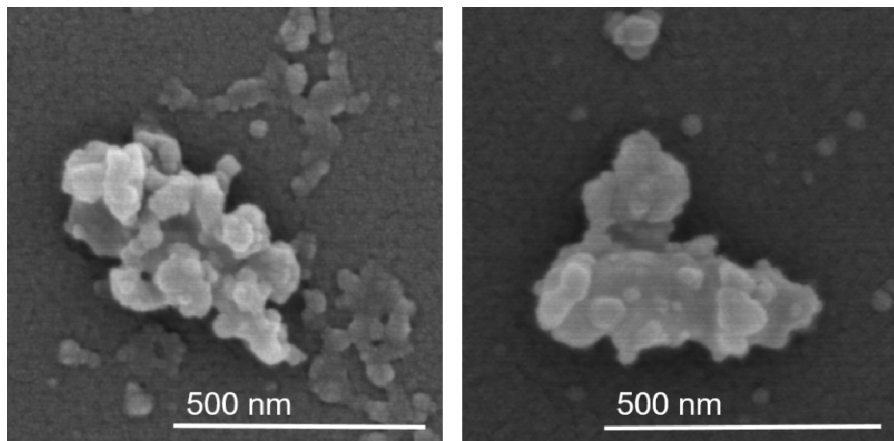


Figure S20 The XPS spectra of Zr-DBDA and Zr-DBDA after treated with epibromohydrin.

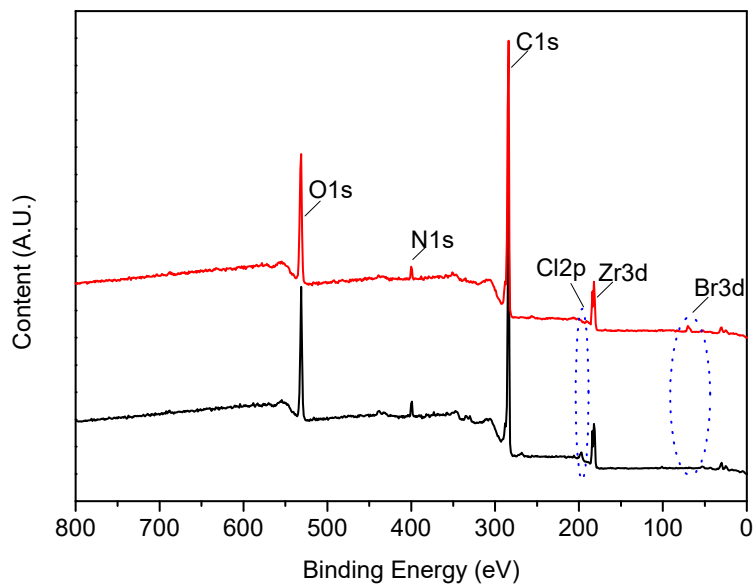


Figure S21 Proposed mechanism of the cycloaddition of CO₂ and epoxides catalyzed by Zr-DBDA.

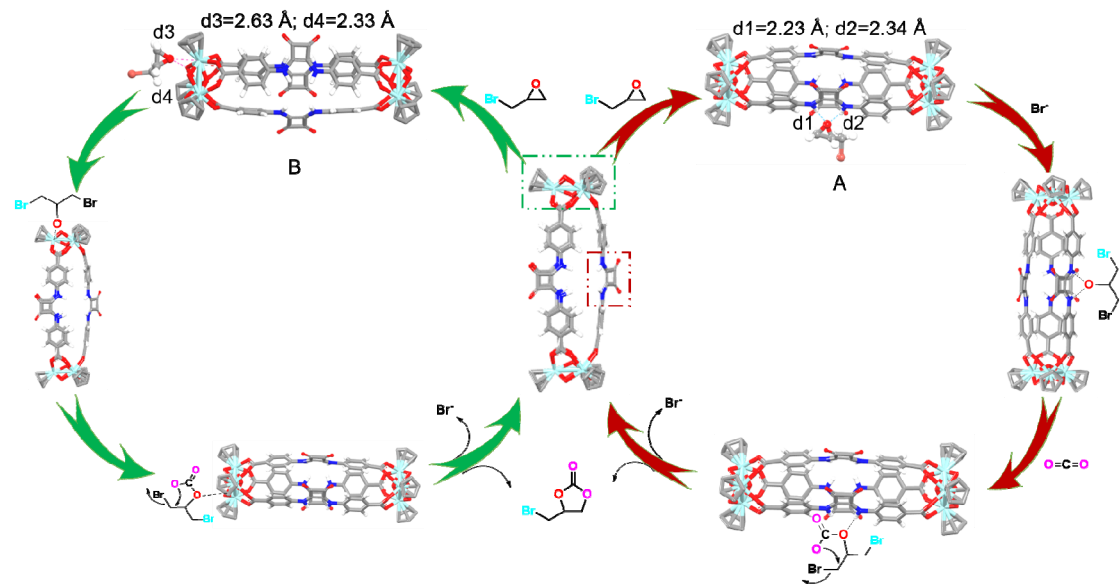


Table S2. Comparison with different porous framework catalysts in the cyclic addition of CO₂ and epibromohydrin under 0.1 MPa CO₂.

Entry	Catalyst	t (hr)	T(°C)	Yield(%)	TON	TOF	Ref.
1 ^a	ImBPDC-Zr	6	120	97	1078	180	S2
4	CNC-Co(III)-Salen	24	25	99	804	33.5	S3
20	[MnL(H ₂ O) ₂]·H ₂ O	36	25	99	893	24.8	S4
6	[Zn(L ₂) ₂]	48	25	93	930	19	S5
7	IPF-CSU-1	48	25	97	97	2	S6
9	CTF-CSU19	48	25	96	-	-	S7
14	N-MOF	48	25	88	17.6	0.37	S8
15	1	48	25	90	225	9.4	S9
16	1·OTf	48	25	85	849.6	17.7	S10
17	COF-PI-2	24	25	13	13	-	S11
18	1	48	25	94.4	-	-	S12
5	[TMGH ⁺][O ₂ MMIIm ⁺][Br ⁻]	20	30	99	4	0.2	S13
21	PRP-1	24	60	85	-	-	S14
1	[Zn(L)(bpa) _{0.5}] _n (1)	6	40	99	100	16.7	S15
2	{[Zn(L)(bpp) _{0.5}]·H ₂ O} _n (2)	6	40	94.8	94.8	15.8	
3	NUC-54	8	60	99	330	41	S16
8	OMe-OH-TPBP-COF	24	40	96	96	4	S17
10	NUC-42	4	60	95	196	49	S18
12	NUC-28	6	60	93	186	31	S19
19	1	12	60	99	35.7	3	S20
	PNU-25-NH ₂	18	55	93	94	5.2	S21
	Zr-DBDA	10	25	99	3510	1345	This work

^aepichlorohydrin instead of epibromohydrin.

Table S3 Comparison with different squaramide-based catalysts in the cyclic addition of CO₂ and epibromohydrin.

Catalyst	Loading	T (°C)	T (hr)	P (MPa)	Yield (%)	TON ^a	TOF ^b	Ref.
SAIL-4	3 mol%	100	3	1.5	98	33	11	S22
15 ^c	2.0 mol%	80	1	1.0	100	85	85	S23
(R)-7 ^d	5.0 mol%	30	24	0.1	81	-	-	S24
PMO-SAF-20 ^d	5 wt%	90	7	2.0	99	-	-	S25
Zr-DBDA	28.5 mmol%	25	10	0.1	99	3510	1345	This work

^aYield of isolated product was calculated by ¹H NMR spectroscopy. ^bMoles of cyclic carbonate per mole of catalyst. ^c1,2-epoxyhexane instead of epichlorohydrin.

^depichlorohydrin instead of epibromohydrin.

Reference

- S1. X. Zhang, Z. Zhang, J. Boissonnault and S. M. Cohen, *Chem. Commun.*, 2016, **52**, 8585.
- S2. Y.-H. Zou, Q.-J. Wu, Q. Yin, Y.-B. Huang and R. Cao, *Inorg. Chem.*, 2021, **60**, 2112.
- S3. L. Hu, Q. Xie, J. Tang, C. Pan, G. Yu and K. Tam, *Carbohydr. Polym.*, 2021, **256**, 117558.
- S4. Y. Yang, C. Gao, H. Tian, J. Ai, X. Min and Z. Sun, *Chem. Comm.*, 2018, **54**, 1758.
- S5. J. Chen, Y. Xu, Z. Gan, X. Peng and X. Yi, *Eur. J. Inorg. Chem.*, 2019, **13**, 1733.
- S6. X. Yu, J. Sun, J. Yuan, W. Zhang, C. Pan, Y. Liu and G. Yu, *Chem. Eng. J.*, 2018, **350**, 867.
- S7. W. Yu, S. Gu, Y. Fu, S. Xiong, C. Pan, Y. Liu and G. Yu, *J. Catal.*, 2018, 1.
- S8. X. Han, X. Wang, P. Li, R. Zou, M. Li and Y. Zhao, *CrystEngComm*, 2015, **17**, 8596.
- S9. P. Li, X. Wang, J. Liu, H. Phang, Y. Li and Y. Zhao, *Chem. Mater.*, 2017, **29**, 9256.
- S10. J. Chen, Z. Gan and X. Yi, *Catal Letters.*, 2018, **148**, 852.
- S11. L. Ding, B. Yao, W. Wu, Z. Yu, X. Wang, J. Kan and Y. Dong, *Inorg. Chem.*, 2021, **60**, 12591.
- S12. J. Lai, Y. Han, H. Li, J. Wang, C. Wang, L. Suo, Y. Sun and K. Wang, *J. Clust. Sci.*, 2020, **31**, 1389.
- S13. J. Hu, J. Ma, H. Liu, Q. Qian, C. Xie and B. Han, *Green Chem.*, 2018, **20**, 2990.
- S14. M. Ding and H. Jiang, *Chem Comm.*, 2016, **52**, 12294.
- S15. Y. Chai, Y. Zhao, X. Liu, Z. Cui, B. Zhao and L. Ma, *Cryst. Growth Des.*, 2022, **22**, 5559.
- S16. H. Chen, T. Zhang, S. Liu, H. Lv, L. Fan and X. Zhang, *Inorg Chem.*, 2022, **61**, 11949.
- S17. F. Yang, Y. Li, T. Zhang, Z. Zhao, G. Xing and L. Chen, *Eur. J. Inorg. Chem.*, 2020, **26**, 4510.
- S18. H. Chen, Z. Zhang, T. Hu and X. Zhang, *Inorg. Chem.*, 2021, **60**, 16429.

-
- S19. T. Zhang, Z. Zhang, H. Chen, X. Zhang and Q. Li, *Cryst. Growth Des.*, 2022, **22**, 304.
- S20. H. Zhou, B. Liu, L. Hou, W. Zhang and Y. Wang, *Chem. Comm.*, 2018, **54**, 456.
- S21. J. F. Kurisingal, Y. Rachuri, Y. Gu, R. K. Chitumalla, S. Vuppala, J. Jang, K. K. Bisht, E. Suresh and D.-W. Park, *ACS Sustainable Chem. Eng.*, 2020, **8**, 10822.
- S22. M. S. Liu, P. H. Zhao, Y. Q. Gu, R. Ping, J. Gao and F. S. Liu, *J. CO₂ Util.*, 2020, **37**, 39.
- S23. S. Sopeña, E. Martin, E. C. Escudero-Adán and A. W. Kleij, *ACS Catal.*, 2017, **7**, 3532.
- S24. K. Takaishi, T. Okuyama, S. Kadosaki, M. Uchiyama and T. Ema, *Org. Lett.*, 2019, **21**, 1397.
- S25. M. S. Liu, P. H. Zhao, R. Ping, F. W. Liu, F. S. Liu, J. Gao and J. M. Sun, *Chem. Eng. J.*, 2020, **399**, 125682.